

Propagating to nonpropagating vibrational modes in amorphous polycarbonate

L. Saviot and E. Duval

Laboratoire de Physico-Chimie des Matériaux Luminescents, UMR-CNRS 5620, Université Lyon I, 69622 Villeurbanne Cedex, France

N. Surovtsev

*Laboratoire de Physico-Chimie des Matériaux Luminescents, UMR-CNRS 5620, Université Lyon I, 69622 Villeurbanne Cedex, France
and Institute of Automation and Electrometry, Russian Academy of Sciences, Novosibirsk, 630090, Russia*

J. F. Jal

Département de Physique des Matériaux, UMR-CNRS 5586, Université Lyon I, 69622 Villeurbanne Cedex, France

A. J. Dianoux

Institut Laue-Langevin, F-38042 Grenoble Cedex, France

(Received 11 December 1998)

Comparisons are made between the low-frequency Raman and inelastic neutron-scattering spectra obtained from amorphous bisphenol A polycarbonate at low temperature. The vibrational density of states and light-vibration coupling coefficient are determined. The frequency dependences of these parameters are explained by propagating vibration modes up to an energy of about 1 meV, and fractonlike modes in more cohesive domains at higher energies. The vibrational dynamics are strongly dependent on disorder in the glass: this disorder comes from fluctuations in bond strengths or elasticity constants, and not from changes in density. [S0163-1829(99)02525-4]

The low-frequency vibrations in glasses and their related thermal properties were first investigated 30 years ago, and are still being studied today. An interesting feature is the excess of vibrational density of states (VDOS) observed by light or neutron inelastic scattering, known as the “boson peak,” and which is responsible for the excess of low-temperature specific heat. This boson peak is universal and observed in polymeric, organic, or inorganic glasses. The characteristics of low-frequency vibrations, occurring approximately in the 0.03–3 THz spectral range, are dependent on the glass structure at the nanometric scale. The problem of glass structure is an old question, which has yet to receive a definite answer.

The principal questions to be answered are the following: Up to what frequency do the vibrational modes propagate and over what distances? What is the origin of the boson peak? Very recently a linear dispersion of the transferred energy versus the transferred momentum was observed by inelastic x-ray scattering (IXS) in several glasses,^{1–4} and in most of them, up to frequencies higher than the position of the boson peak. Such a linear dispersion is, *a priori*, characteristic of propagating modes. However, it was shown that a linear dispersion can also be explained by nonpropagating modes in a heterogeneously bonded network at the nanometric scale.⁵ In fact, today, the propagating or nonpropagating character of vibrational modes in the boson peak is not definitively established, as the origin of the boson peak is not completely known. It is clear enough that the fluctuations of bonding or of elastic constants are the cause of the excess of VDOS.^{6–8} But we face the problem of the fluctuations which are either homogeneously distributed in a continuous random network, or inhomogeneously distributed in a network built of nanometric domains characterized by strong cohesion, which are separated by softer zones.^{6,7} This latter glass de-

scription is consistent with the existence of cooperatively rearranging regions,^{9–11} dynamical heterogeneities,¹² or frustration-limited domains¹³ in the supercooled state.

The comparison between inelastic light and neutron scatterings allows the VDOS and the light-vibration coupling coefficient to be determined. These two physical parameters contain information on the characteristics of the vibrational modes and on the structure of the vibrating network. They are not known with a sufficient precision for harmonic vibrations at frequency lower than the boson peak, because at a temperature which is not very low, the corresponding scattering is masked by the contribution from anharmonic or relaxational modes.^{7,14} In general, even if the temperature of glass transition (T_g) is high, as for silica,¹⁵ the scattering from anharmonic modes is non-negligible down to 50 K. Measurements must therefore be made at low temperatures, where the scattering is weak. To study the harmonic vibrations at low-frequency, we chose the bisphenol A polycarbonate (PC), which gives a relatively strong scattering from harmonic modes at low-frequency and low temperature.

In this paper we present the experimental results of light and neutron scattering. We will consider particularly the scattering from harmonic vibrations. The problem of relaxational motions in PC was dealt with in another paper.¹⁴ The characteristics of vibrational modes, the nature of disorder, and the nanometric structure will be discussed in the light of the experimental results.

The PC specimen was purchased from Bayer. The number average molecular weight is 15 600 mol⁻¹ with a polydispersity index of 1.85. The glass transition temperature is around 420 K, as determined by differential scanning calorimetry.

The polarized and depolarized low-frequency Raman light scattering (LFRS) were analyzed with a high-resolution and

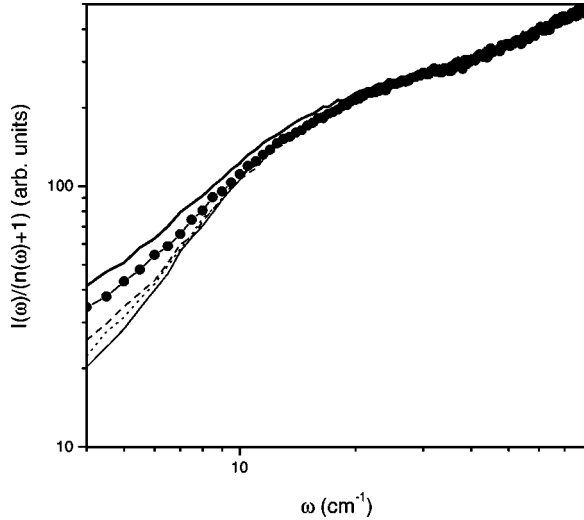


FIG. 1. Reduced low-frequency Raman scattering at different temperatures: 15 K (thin line), 26 K (dotted line), 53 K (dashed line), 108 K (black circles), and 139 K (thick line).

high-contrast five grating monochromator (Dilor Z40). The $\lambda = 752.5$ nm line of the krypton laser was used to avoid the luminescence. The scattering was observed along a direction, perpendicular to the laser beam. The spectra were taken at different temperatures, using a helium flow cryostat up to room temperature and a furnace for higher temperatures.

The inelastic neutron spectra were recorded on the time-of-flight instrument IN6 at the ILL, Grenoble. The wavelength of the incident neutrons was equal to 5.12 \AA^{-1} resulting in an elastic resolution full width at half maximum of $80 \text{ } \mu\text{eV}$, and a momentum transfer range extending from $Q = 0.22 \text{ \AA}^{-1}$ to $Q = 2.06 \text{ \AA}^{-1}$. The spectra were taken in the temperature interval 15–390 K, using a helium cryofurnace. The scattering cross sections were obtained after the usual standard calibrations by means of the vanadium runs, and removal of contributions from empty cans. On the basis that PC mainly yields incoherent scattering (as was experimentally checked), we calculated the total density of states through the use of an iterative procedure described elsewhere.¹⁶ The density of states obtained in this way was corrected by the Debye-Waller factor and for the multiphonon contributions.

The reduced LFERS intensity, that is the intensity divided by the Bose factor plus one for Stokes scattering, i.e., $I(\omega)/[n(\omega)+1]$, is plotted in Fig. 1 against the frequency ω . It can be observed that the scattering increases at low energy with temperature. This is due to the increase of the density of anharmonic or relaxational modes, which is negligible at temperature $T \leq 30$ K. In this plot, the boson peak corresponds to the shoulder which appears in the $10\text{--}20 \text{ cm}^{-1}$ spectral interval.

The INS from anharmonic modes was found to be negligible up to $T = 30$ K. By comparison of the scattering intensities at the two lowest temperatures, $T = 15$ K and $T = 30$ K, knowing that the INS from harmonic modes is proportional to the Bose factor, it was possible to determine accurately the VDOS for harmonic vibrations at 15 and 30 K, in the spectral range $2\text{--}80 \text{ cm}^{-1}$. The VDOS at different temperatures is plotted against frequency in Fig. 2. As for the LFERS intensity, the VDOS at low frequency increases with

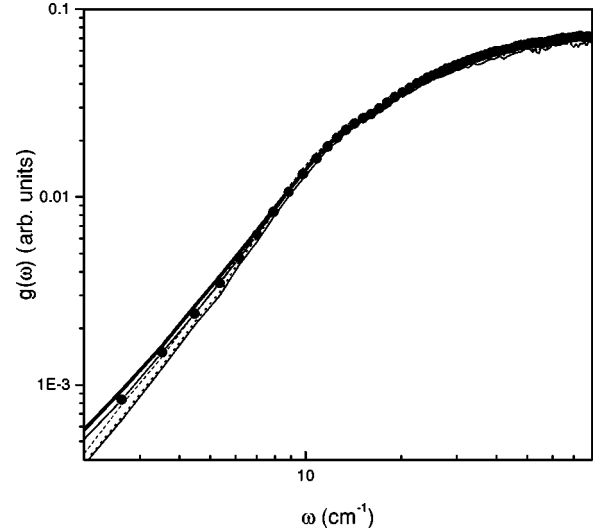


FIG. 2. Vibrational density of states deduced from inelastic neutron scattering at different temperatures: 15 K (thin line), 30 K (dotted line), 50 K (dashed line), 110 K (black circles), and 140 K (thick line).

temperature, together with the density of anharmonic modes. The shoulder, which corresponds to the boson peak, appears in the same spectral range ($10\text{--}20 \text{ cm}^{-1}$) as for LFERS.

The deduced VDOS $g(\omega)$ is summed over the different types of modes, which are specified by the subscript i :

$$g(\omega) = \sum_i g_i(\omega). \quad (1)$$

The LFERS intensity for the i modes is proportional to the VDOS $g_i(\omega)$, multiplied by the light-vibration coupling coefficient $C_i(\omega)$, i.e.,

$$\frac{I(\omega)\omega}{n(\omega)+1} = \sum_i C_i(\omega)g_i(\omega). \quad (2)$$

An effective light-vibration coupling coefficient $C(\omega)$ is generally used. It is defined by the following equation:

$$\frac{I(\omega)\omega}{n(\omega)+1} = C(\omega)g(\omega). \quad (3)$$

At 15 and 30 K, the lowest temperatures at which the INS was observed, the contribution of anharmonic modes is negligible, so that the measured VDOS is due only to harmonic modes. It is observed in Fig. 2 that, at the lowest frequencies, in the $2\text{--}6 \text{ cm}^{-1}$ spectral range, the VDOS has an ω^2 -frequency dependence, as in the Debye regime for acoustic vibration modes. At higher frequencies, at the foot of the boson peak, the frequency dependence increases, then decreases beyond $\omega = 12 \text{ cm}^{-1}$. From $20\text{--}60 \text{ cm}^{-1}$, a frequency dependence close to $\omega^{0.6}$ is observed.

From the Raman intensity (Fig. 1) and the VDOS (Fig. 2), the effective light-vibration coupling coefficient $C(\omega)$ can be calculated. It is plotted in Fig. 3. At low frequency $C(\omega)$ is insensitive to thermal variation up to 80 K. It increases noticeably above 140 K, when light couples with relaxational motions. The corresponding coupling coefficient is confirmed to be frequency independent.¹⁵ Even at low tempera-

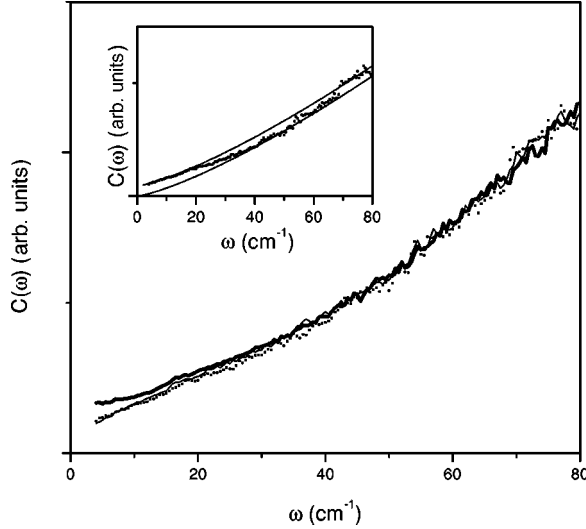


FIG. 3. Light-vibration coupling coefficient at three temperatures: 15 K (thin line), 30 K (dotted line), and 140 K (thick line). In the inset $C(\omega)$, at $T = 30$ K, is plotted in the same spectral interval, and compared with $\omega^{1.3}$ or $\omega^{1.3} + \text{const}$.

ture, $C(\omega)$ goes progressively from a constant C_1 , at the lowest frequencies, to $C_2(\omega) \sim \omega^{1.3}$ at frequencies higher than 30 cm^{-1} (see the inset in Fig. 3). As there is no obvious variation of the constant C_1 from 15–50 K, and given that the contribution of anharmonic modes to the VDOS is negligible up to this temperature, we deduce that C_1 is attributable to the lowest harmonic modes.

In a phenomenological model, the frequency dependence of $g(\omega)$ and $C(\omega)$, at the lowest temperatures (Figs. 2 and 3) can be described by the presence of two different types of harmonic modes: (1) modes which are characterized by $C_1(\omega) = C_1 = \text{const}$ (at very low frequency); these correspond mostly to frequencies lower than the boson peak; (2) modes corresponding to $C_2(\omega) \sim \omega^{1.3}$ and $g_2(\omega) \sim \omega^{0.6}$.

Comparison of Fig. 2 with Fig. 3, reveals that the frequency independent coupling coefficient C_1 is for the harmonic vibration modes, which have a ω^2 -dependent VDOS at the lowest frequencies. In this Debye regime the modes are expected to have a propagating character. The propagation of these Raman-active vibrations is attenuated because of glass disorder, which is characterized by a radial correlation length in the isotropic (at the considered scale) disordered medium.¹⁷ The characteristic damping length is shorter than the light wavelength, and longer than the vibration wavelength. In determining $C_1(\omega)$ for the damped propagating modes, it is assumed that the fluctuations of susceptibility at the origin of Raman scattering are only due to the fluctuations of vibrational wave function.¹⁷ In other words, it is assumed that the Raman scattering is due to the mechanical disorder.¹⁸ If the vibrational wave function is $\psi(\mathbf{r}, \omega)$, with \mathbf{r} the position vector, the expression of $C_1(\omega)$ is¹⁷

$$C_1(\omega) \propto \int \int_{-\infty}^{\infty} d\mathbf{R} d\mathbf{r} \nabla \psi(\mathbf{R}, \omega) \nabla \psi^*(\mathbf{R} + \mathbf{r}, \omega). \quad (4)$$

With $\psi(\mathbf{R}, \omega)$ a normalized wave function and \mathbf{k} the wave vector of the propagating vibration, one obtains

$$C_1(\omega) \propto (k^2 + \xi^{-2}) \int_{-\infty}^{\infty} e^{i\mathbf{k} \cdot \mathbf{r}} e^{-r/\xi} d\mathbf{r}, \quad (5)$$

where ξ is the radial correlation length of the propagating mode. The Fourier transform (5) is²⁰

$$C_1(\omega) \propto \frac{8\pi\xi^{-1}}{(k^2 + \xi^{-2})}. \quad (6)$$

For a correlation length longer than the vibration wavelength ($\xi > k^{-1}$),

$$C_1(\omega) \propto \frac{\xi^{-1}}{k^2}. \quad (7)$$

As shown in Ref. 17, the disorder in isotropic glasses is described by two correlation lengths: radial and angular. The angular disorder, which is related to the disorder in the bond angles, is in general characterized by a short correlation length ($< 1 \text{ nm}$),¹⁷ and consequently has certainly no effect on the considered acoustic propagating modes, whose wavelengths are longer than 2 nm. At this point it is interesting to compare our results with the inelastic x-ray scattering (IXS) measurements. A linear dispersion $\omega(k)$ was observed in several glasses, which leads to an effective velocity of sound, which is close to the macroscopic longitudinal one.^{1–4} At frequencies lower than the boson peak, the IXS is certainly due to propagating modes. The width of the IXS peak was also found to have a k^2 dependence,^{1,2} as in classical Brillouin scattering. Since it has been confirmed²¹ that the same modes are observed in LFRS, INS, and IXS, the IXS peak width is inversely proportional to the inverse of correlation length ξ^{-1} . In consequence, $\xi^{-1} \propto k^2$ and finally $C_1(\omega) = \text{const}$. There is a consistency between light, neutron, and x-ray scatterings, showing that there is a propagation of acoustic modes, at least along a distance equal to ξ , at frequencies lower than the boson peak.

It has been shown that in a one-dimensional (1D) system, with a disorder of bonding or of elastic constants, the localization length was proportional to ω^{-2} .^{22,23} This frequency behavior was confirmed numerically.²⁴ It is expected that in a 3D system the radial correlation length, which is related to the disorder along one dimension, has also a ω^{-2} dependence. The conclusion is that the disorder in glasses is principally characterized by fluctuations of bond strength or of elastic constants. This hypothesis is confirmed by the frequency independent $C(\omega)$, which was recently deduced from the comparison of LFRS with INS for silica glass.²⁵ From another point of view the ω^{-2} dependence of the localization length can be explained by an anharmonic coupling between propagating phonons and localized vibrational excitations.^{26,27}

Above 7 cm^{-1} , the frequency dependence of the VDOS becomes more rapid than ω^2 (Fig. 2) at the foot of the boson peak, or, from another point of view, at the limit of the Brillouin zone of a quasiperiodic system. In agreement with the model of inhomogeneous nanometric bonding, the glass is built of more cohesive domains separated by softer zones.^{28,6,7} The arrangement of domains is quasiperiodic, but obviously the periodicity is blurred, in particular because there exists a more or less broad size distribution of domains.

As expected the VDOS has a frequency dependence, which becomes more rapid than ω^2 when the Brillouin-zone limit of the quasiperiodic arrangement is approached.

The modes which are observed at frequencies higher than the boson peak, between $\sim 20 \text{ cm}^{-1}$ and $\sim 60 \text{ cm}^{-1}$ (Figs. 2 and 3), correspond to $g_2(\omega) \sim \omega^{0.6}$, and $C_2(\omega) \sim \omega^{1.3}$. These respective frequency dependences are close to the ones observed in poly(methylmethacrylate) (PMMA), and the same interpretations, as for this polymeric glass, can be proposed. The VDOS is proportional to $\omega^{\tilde{d}-1}$, where \tilde{d} is a spectral dimension. From experiment, $\tilde{d} \approx 1.6$. It was also shown that $C_2(\omega) \sim \omega^{2\tilde{d}/D}$, where D is a fractal dimension, if the radial correlation length is equal to or shorter than the localization length, and the angular correlation length shorter than the localization length.¹⁷ Therefore $D \approx 2.5$. From this interpretation it follows that the structure in cohesive domains is that of a disordered fractal. The same conclusions were obtained for PMMA. The value of \tilde{d} and D are in good agreement with a percolative system slightly above the threshold.²⁹

From this model, which is equivalent to the one described in previous papers,^{28,6,7} the mean size of domains or percolating clusters is $2a \approx v/\omega_B c$, where ω_B is the frequency (cm^{-1}) of the boson peak, c the vacuum speed of light, and v the sound velocity. From the Raman depolarization coefficient, that is close to 0.75, it follows that the vibrational modes are transversal or torsional.¹⁸ This is confirmed by the identical temperature dependence found in PC for ω_B and for the transverse sound velocity in PC.¹⁹ Taking for the macroscopic transverse sound velocity $v = 1100 \text{ m/s}$, for $\omega_B = 12 \text{ cm}^{-1}$, it is found $2a = 3 \text{ nm}$. This value is very close to the size of dynamical clusters,¹² coherent domains,⁹⁻¹¹ or frustration-limited domains¹³ in the supercooled state.

Returning to the comparison with the IXS, we remark that

a linear $\omega(k)$ dispersion is observed even at frequencies close to or higher than the boson peak.^{1,2,4} This does not contradict the interpretation presented in this paper. Indeed, it was shown very recently that a linear dispersion can be observed in IXS by nonpropagating modes.⁵ In this model the modes involved in IXS are the fundamental vibration modes of cohesive domains. As mentioned above, the frequency of these modes is inversely proportional to the domain size, which is inversely proportional to the transferred momentum k . Furthermore, there is a correlation between neighboring domains, the correlation length is proportional to ω^{-2} in our model. That explains, on the one hand, the observed linear dispersion up to frequencies for which the propagation of modes is generally not expected, and, on the other hand, the ω^2 dependence of the width of the IXS peak.

The comparison between low-frequency Raman scattering and inelastic neutron scattering, at low temperature, provides a clear vision of the vibrational dynamics and of the nanoscopic structure of polymeric glasses. In polycarbonate, at frequencies lower than 7 cm^{-1} ($\approx 1 \text{ meV}$) the vibrations are acoustic propagating modes characterized by a correlation length, which is proportional to the inverse of the square of the frequency (ω^{-2}). In consequence the light-vibration coupling coefficient is frequency independent; this has been experimentally verified. The frequency dependence of the correlation length is in agreement with a glass network, in which the bonding is disordered. In fact there exist principally fluctuations of elastic constants rather than density fluctuations. This description is consistent with the $\omega(k)$ linear dispersion, observed by IXS from propagating modes for frequencies lower than the boson peak, and with the width of the IXS peak, which is proportional to the square of the momentum transfer. The disordered bonding network is considered as built of nanometric cohesive domains separated by softer zones.

-
- ¹C. Masciovecchio *et al.*, Phys. Rev. Lett. **76**, 3356 (1996).
²P. Benassi *et al.*, Phys. Rev. Lett. **77**, 3835 (1996).
³M. Foret *et al.*, Phys. Rev. Lett. **77**, 3831 (1996).
⁴A. Mermet *et al.*, Phys. Rev. Lett. **80**, 4205 (1998).
⁵E. Duval and A. Mermet, Phys. Rev. B **58**, 8159 (1998).
⁶A. Mermet *et al.*, Polymer **37**, 615 (1996).
⁷A. Mermet *et al.*, Europhys. Lett. **36**, 277 (1996).
⁸W. Schirmacher *et al.*, Phys. Rev. Lett. **81**, 136 (1998).
⁹G. Adam and J. H. Gibbs, J. Chem. Phys. **43**, 139 (1965).
¹⁰E. Donth, J. Non-Cryst. Solids **53**, 325 (1982).
¹¹C. T. Moynihan and J. Schroeder, J. Non-Cryst. Solids **160**, 52 (1993).
¹²U. Tracht *et al.*, Phys. Rev. Lett. **81**, 2727 (1998).
¹³D. Kivelson *et al.*, Physica A **219**, 27 (1995).
¹⁴L. Saviot, E. Duval, J. F. Jal, and A. J. Dianoux (unpublished).
¹⁵A. P. Sokolov *et al.*, Phys. Rev. B **52**, R9815 (1995).
¹⁶A. Fontana *et al.*, Phys. Rev. B **41**, 3778 (1990).
¹⁷E. Duval *et al.*, J. Chem. Phys. **99**, 2040 (1993).
¹⁸V. N. Novikov *et al.*, J. Chem. Phys. **102**, 4691 (1995).
¹⁹V. N. Novikov *et al.*, J. Chem. Phys. **107**, 1057 (1997).
²⁰J. Jackle and K. Frobose, J. Phys. F **9**, 967 (1979).
²¹C. Masciovecchio *et al.*, Philos. Mag. B (to be published).
²²A. Crisanti, G. Paladin, and A. Vulpiani, *Products of Random Matrices in Statistical Physics* (Springer, Berlin, 1992).
²³J. M. Luck, *Systèmes Désordonnés Unidimensionnels* (Alea, Saclay, 1992).
²⁴M. Montagna, G. Ruocco, G. Viliani, R. Di Leonardo, R. Dusi, G. Monaco, M. Sampoli, and T. Scopigno (private communication).
²⁵A. Fontana, R. Dell'Anna, M. Montagna, F. Rossi, G. Viliani, G. Ruocco, M. Sampoli, U. Buchenau, and A. Wischniewski, Europhys. Lett. (to be published).
²⁶A. Jagannathan *et al.*, Phys. Rev. B **39**, 13 465 (1989).
²⁷R. Vacher *et al.*, Phys. Rev. B **56**, R481 (1997).
²⁸E. Duval *et al.*, J. Phys.: Condens. Matter **2**, 10 227 (1990).
²⁹A. Rahmani *et al.*, J. Phys.: Condens. Matter **5**, 7941 (1993).